JOURNAL OF AIRCRAFT
Vol. 37, No. 5, September–October 2000

Reduced-Order Dynamic Aeroelastic Model Development and Integration with Nonlinear Simulation

B. A. Winther,* P. J. Goggin,† and J. R. Dykman‡
The Boeing Company, Long Beach, California 90807

Piloted and batch simulations of the aeroservoelastic response are essential tools in the development of advanced flight control systems. In these simulations the number of differential equations must be sufficiently large to yield the required accuracy, yet small enough to enable real-time evaluations of the aircraft flying qualities. The challenge of these conflicting demands is reinforced by nonlinearities in the quasi-steady equations of motion and by the complex characteristics of the oscillatory forces. Our solution to the problem is based on a unique formulation that eliminates the need for auxiliary state variables to represent the unsteady aerodynamics. We also address transformations from the mean flight path axes to a body axes coordinate system and describe how the structural dynamic equations of motion are integrated with the quasi-steady, nonlinear, six-degree-of-freedom plant model. The unified model, which accurately preserves the roots of the dynamic aeroelastic system, includes provisions for control surface inputs and atmospheric turbulence.

Nomenclature

A, B	=	matrices in state-space formulation
$\boldsymbol{e}$	=	vector of generalized body axes coordinates
F_m	=	aerodynamic generalized force
f, g, h	=	aircraft displacements in mean flight path system
G_{NL}	=	solution to nonlinear six-degree-of-freedom equations
M_m	=	inertial generalized force
$\boldsymbol{P}$	=	vector derived in p transform
p, q, r	=	aircraft angular rates about body axes
$\bar{q}$	=	dynamic pressure
S_m	=	structural generalized force
T	=	transformation matrix
U	=	mean airflow velocity
u, v, w	=	aircraft linear rates along body axes
X, Y, Z	=	aircraft mean flight path axes system
$\bar{X}, \bar{Y}, \bar{Z}$	=	aircraft body axes system
$\boldsymbol{z}$	=	state variable vector in body axes system
$\alpha_{m,n}$	=	real part of aerodynamic approximation
$\beta_{m,n}$	=	imaginary part of aerodynamic approximation
$\gamma_{m,n}$	=	element of structural damping matrix
ΔG	=	linear equations added to G_{NL}
δ	=	vector of inputs
ε	=	vector of generalized mean flight path coordinates
$\boldsymbol{\eta}$	=	state variable vector in mean flight path system
$\kappa_{m,n}$	=	element of structural stiffness matrix
λ	=	complex eigenvalue
$\mu_{m,n}$	=	element of mass matrix
σ	=	real part of eigenvalue
Φ_I	=	imaginary part of eigenvector
Φ_R	=	real part of eigenvector
ω	=	circular frequency

Subscripts

m, n	=	modal indices
NL	=	nonlinear quantity

Superscripts

$\cdot$	=	$\mathrm{d}(\ )/\mathrm{d}t$
T	=	transposed matrix

Introduction

MANY recent aircraft designs use digital flight control systems for stability and control. A goal in the development of these systems that include autopilots, yaw dampers, stability augmentation systems, and wing levelers is to ensure that the aircraft structural performance is maintained at all operational flight conditions. In this context, structural performance is defined in terms of the aeroelastic stability and the structural loads caused by maneuvers and atmospheric turbulence.

In the past, the flight control systems were designed by accounting for the quasi-steady stability of the aircraft. Typically this was performed by the use of six-degree-of-freedom (6-DOF) simulations. Many times these simulations became quite complex and included elastic effects as well as nonlinear phenomena, for example aerodynamic, hydraulic, structural, that were considered important in the flight control design. A refinement that accounted for aircraft body axes rotations relative to its mean axes was developed by Rodden and Love[1] for the unaugmented aircraft and by Winther et al.[2] for a control configured system.

As the control systems were designed, they were incorporated with the dynamic aeroelastic model of the aircraft and the structural performance was evaluated. The dynamic aeroelastic models used in the evaluation were identical to the ones developed for flutter analysis (in the following referred to as flutter models) that generally sacrificed accuracy of the quasi-steady aircraft response in return for consideration of the structural dynamics. The reduced accuracy in the quasi-steady solution was caused by many modeling assumptions, such as small structural displacements, linear hydraulics, and linear aerodynamics based on potential flow theory. Any degradation in the structural performance was remedied by modification of the control system in a trial-and-error fashion. Usually this was accomplished by applying notch filters that reduced the gain of the control system in the adversely affected frequency band.

Modern aircraft designs often incorporate control systems that interact with the response of the airframe elastic modes, as well as with the rigid-body response. Applications include gust and maneuver

Presented as Paper 98-1897 at the AIAA/ASME/ASCE/AHS/ASC 39th Structures, Structural Dynamics, and Materials Conference, Long Beach, CA, 20–23 April 1998; received 14 July 1998; revision received 15 December 1999; accepted for publication 31 January 2000.

*Senior Principal Engineer, Airlift and Tanker Loads and Dynamics. Associate Fellow AIAA.
†Director, Structures Technology—Long Beach. Senior Member AIAA.
‡Principal Engineer, Airlift and Tanker Stability, Control and Flying Qualities. Member AIAA.

load alleviation, elastic mode control, ride quality augmentation, and flutter suppression. Examples of aircraft equipped with one or more of these complex control systems date back to the L-1011 commercial transport and now include the B-1 bomber, the B-2 bomber, the F/A-18C/D attack and fighter aircraft, the A-320 commercial transport, and the B-767 commercial transport. Depending on the control application, the systems were designed by applying either the quasi-steady aeroelastic model or the flutter model.

Future design concepts like the High Speed Civil Transport (HSCT) and the Blended Wing Body (BWB) aircraft involve a significant advancement in flight controls technology. Systems including load alleviation as well as elastic mode control are considered for these types of transport aircraft for which affordability is the main driver in the design process. Both of the proposed designs (HSCT and BWB) are extremely lightweight and flexible compared with traditional aircraft. The increase in flexibility means that the frequency separation between the quasi-steady and the structural response is reduced. To describe the dynamics in this situation adequately, the analyst needs to apply the most accurate plant models available. The models should include an accurate representation of both the mean axis aircraft response and the structural dynamic response. As indicated earlier, the most accurate mean axis response generally is obtained from the 6-DOF nonlinear quasi-steady aircraft equations of motion (QSAE) and the most accurate structural dynamic response is obtained from the flutter model.

Piloted simulations as well as batch analyses are required in the development of advanced control systems. The combined QSAE and dynamic aeroelastic plant model must be sufficiently large to yield the required accuracy, yet small enough to enable real-time pilot evaluations and rapid batch simulations for control law design. This requirement becomes even more challenging when one considers the complex characteristics of the unsteady aerodynamics and the nonlinear behavior of the QSAE model. Any increase in the number of equations representing the unsteady aerodynamics translates directly into a reduction in the number of structural dynamic degrees of freedom that can be considered.

This paper presents a technique that has been developed to meet these somewhat conflicting requirements. The technique is based on a unique formulation of the structural dynamic equations that eliminates the requirement for auxiliary states to represent the unsteady aerodynamics. We also address transformations from the mean flight path axes to a body axis coordinate system and the integration of the structural dynamic equations with the QSAE model. This unified model preserves the aeroelastic trim solution and provides the appropriate structural dynamic effects. Model inputs include control surface motion as well as atmospheric turbulence.

Theoretical Development

The flutter model equations of motion (EOMs) are generally solved in the frequency domain. This is because of the computational efficiency associated with the solution in this domain and the fact that the aerodynamic forces generally are computed as functions of frequency. Development of techniques to transfer the flutter model EOMs from the frequency domain to the time domain has been researched for many years. This research includes the work performed by Sevart,[3] Vepa,[4] Edwards,[5] Roger,[6] and Richardson,[7] using Padé approximants and so-called rational function approximations (RFAs). The Padé approximants and RFAs are known to add a significant number of aerodynamic lag equations to the overall aircraft equations of motion. Typically, for a 20-mode solution the added number of equations could exceed 80.

Karpel[8] presented a technique called the "minimum state" RFA. This technique takes advantage of the aerodynamic lag equations that produce a sparsely populated matrix when coupled into the equations of motion. An iterative procedure is used to calculate the aerodynamic lag states and the associated state-space matrices. The number of aerodynamic states is generally much smaller than that required in the previously discussed RFA method and it is not directly dependent on the number of structural degrees of freedom. One of the drawbacks of the Karpel approach is that the iterative procedure sometimes converges slowly and can be time-consuming to perform.

Pitt and Goodman[9] described a method that is somewhat reminiscent of our method in that it does not require any auxiliary lag states. Their technique is based on calculating an equivalent analytical approximation that matches a selected frequency response. It incorporates linear and nonlinear fitting procedures to improve the state-space model using a transition matrix that may be derived from the p-k flutter solution.

Past developments of time domain representations were focused on the aircraft motion induced aerodynamics. However, to obtain a general time domain model, gust force excitations also must be represented in an accurate manner. Applications of the RFAs in Refs. 3–8 can result in considerable errors in the derived gust forces, especially for large transport aircraft that have significant gust penetration effects. Dykman[10] developed an explicit time-lagged, repeated root RFA that accurately describes the gust forces (including the gust penetration delay). This method was evaluated and modified for efficiency by Goggin.[11] The modifications included the use of optimization techniques for selecting gust lag states that were constrained to a common set for the complete aeroelastic system.

Related research on minimum state aeroelastic models has also been performed using eigenmodes and singular value decomposition of the aerodynamic system. Hall,[12] Florea and Hall,[13] and Romanowski and Dowell[14] investigated a technique that generates a reduced-order model of the system from the aerodynamic eigenmodes. Baker et al.[15] applied a similar approach using singular value decomposition and internal balancing to reduce the number of states even further by considering only the states that are important for observability and controllability of the aerodynamic system. Although this work was focused primarily on reduction of high fidelity aerodynamic analyses (like computational fluid dynamic solutions), it could be applied to the present type of problem in which the aerodynamic forces are derived from a less elaborate method, such as the doublet lattice method.[16,17]

To yield a usable batch and real-time simulation capability, the combined QSAE and dynamic aeroelastic plant equations must be formulated and solved in an efficient manner. The addition of computational states lead to considerable increases in computing time and data storage requirements. Thus, with computational efficiency being a pacing constraint, a reduction in the number of aerodynamic lag terms allow an equivalent increase in the number of structural dynamic degrees of freedom that can be added to the simulation.

Heimbaugh[18] developed a formulation that generates an accurate solution of the aeroelastic EOMs without any associated aerodynamic lag terms. The formulation is analogous to the process employed in structural dynamics to reduce the number of degrees of freedom and transform the equations into modal coordinates using the Galerkin[19] method. Heimbaugh applied the so-called p-k flutter solution technique to decouple the aircraft EOMs. Each solution is iterated upon until the assumed aerodynamic frequency coincides with the frequency of the associated aeroelastic mode. Partitions of the orthogonalized (decoupled) state matrix and the corresponding input/output matrices are retained for each converged mode.

In this paper we present an efficient method that is based on Heimbaugh's technique. We enhance this technique by linking the dynamic aeroelastic EOMs with the nonlinear 6-DOF equations that are used in batch and piloted simulations. The core of the simulation[20] is a mathematical model represented by the equation

$$\dot{z}_{\mathrm{NL}} = G_{\mathrm{NL}}(z_{\mathrm{NL}}, \dot{z}_{\mathrm{NL}}, \delta_{\mathrm{NL}}) \tag{1}$$

where z_{NL} denotes an array of state variables describing the aircraft motion. The function G_{NL} represents the nonlinear 6-DOF equations that are derived from an aerodynamic database as well as from models of the atmosphere, aircraft mass distribution, engine performance, and actuator characteristics. The initial conditions are computed using a constrained nonlinear optimization process that determines the equilibrium point where selected trim-to z_{NL} response values are generated from a set of trim-with δ_{NL} variables. The equilibrium point is referred to as the trim point, although nonzero accelerations may be specified in the z_{NL} vector. Each selected output represents one degree of freedom or one constrained equation of motion. The trim procedure may constrain a maximum of 11 equations defining three linear accelerations, three angular accelerations, aircraft velocity, rate of climb, side-slip, roll rate, and pitch rate. The δ_{NL} set contains the control surface deflections.

Aircraft structural dynamics is modeled by adding the unsteady part of the linear equations to the nonlinear simulation in the following manner:

$$\dot{z} = G_{NL} + \Delta G_A z + \Delta G_B \delta \tag{2}$$

where z denotes a state vector that combines z_{NL} with the structural degrees of freedom. Similarly, δ represents a vector of input variables.

In the next section we will discuss the linear structural response equations that are formulated using a method that we refer to as the minimum state p-transform representation. The intent is to identify the dynamic and the quasi-steady components of these linear equations and then replace the quasi-steady portion (QSAE) with the G_{NL} function supplied by the nonlinear 6-DOF simulation. The nonlinear model thus will be coupled with linear terms representing the dynamic degrees of freedom. Because structural flexibility is accounted for in the nonlinear simulation, the elastic contribution from the retained dynamic modes needs to be subtracted from the QSAE, so that the quasi-steady characteristics are preserved in the combined EOMs. Speed- and altitude-dependent terms for the dynamic degrees of freedom may be obtained at each time step by explicitly representing these terms in the EOMs or by interpolating matrices that are precomputed and stored in a database. The range of interpolation remains to be determined.

Discussion of Dynamic EOMs

In the discipline of structural dynamics and flutter it is customary to define the aircraft motion in a mean flight path (MFP) axes system (X, Y, Z), where X is positive aft, Y positive starboard, and Z positive up. This system is aligned with the unperturbed flight path and moves with the average (initial) velocity of the aircraft relative to an Earth-fixed system. Transformations between the MFP axis system and the Earth-fixed system are defined in Ref. 2, Eq. (1). In nearly all flutter analyses the aircraft is assumed to be in equilibrium, horizontal flight, and only small displacements relative to the MFP axes are considered. The equations then may be written in the following form:

$$M_m + S_m = \bar{q} F_m \tag{3}$$

The terms on the left-hand side are defined by

$$M_m = \sum_{n=1}^{N} \mu_{m,n} \ddot{\varepsilon}_n, \qquad S_m = \sum_{n=4}^{N} (\kappa_{m,n}\varepsilon_n + \gamma_{m,n}\dot{\varepsilon}_n) \tag{4}$$

The aerodynamic generalized forces F_m depend on Mach number and frequency. Several methods are available for transforming the EOMs into the time domain by replacing these forces with a set of approximating functions as discussed in the preceding section. The method originally developed by Heimbaugh was selected as the most promising for the present application. It can be characterized as a minimum state representation of the generalized aerodynamic forces because it does not require lag states commonly associated with other methods. As noted, the method is analogous to the eigenvector reduction technique that is used to orthogonalize modes in structural vibration analyses. The resulting uncoupling of the aeroelastic modes means that the generalized forces associated with each mode need to be accurate only in a relatively narrow frequency band. It is our experience that first-order, quasi-unsteady representations of the aerodynamic forces F_m:

$$F_m(\omega) \approx \sum_{n=1}^{N} (\alpha_{m,n}\varepsilon_n + \beta_{m,n}\dot{\varepsilon}_n) \tag{5}$$

are sufficient. The fit frequency for mode n matches the estimated frequency ω_n of the nth eigenvalue as described later. The aerodynamic force approximation is combined with structural stiffness and damping terms yielding a set of first-order differential equations that may be expressed in the following canonical form:

$$\dot{\eta} = \bar{A}(\omega)\boldsymbol{\eta} + \bar{B}(\omega)\delta \tag{6}$$

where the transposed state vector is defined by

$$\boldsymbol{\eta}^T = (\dot{\varepsilon}_1, \dot{\varepsilon}_2, \ldots, \dot{\varepsilon}_N, \varepsilon_1, \varepsilon_2, \ldots, \varepsilon_N) \tag{7}$$

The roots $\lambda = (\sigma \pm i\omega)$ and eigenvectors $\Phi = (\Phi_R \pm i\Phi_I)$ are obtained by solving

$$(\lambda I - \bar{A})\Phi = 0 \tag{8}$$

This equation is solved in an iterative manner to ensure that the fit frequency for the aerodynamic approximation matches the eigenvalue solution frequency ω_n. At each of these frequencies a new set of equations

$$\dot{P} = \hat{A}\boldsymbol{P} + \hat{B}\delta \tag{9}$$

is obtained by performing the following transformation (sometimes referred to as the p transform):

$$\boldsymbol{\eta} = \bar{T}\boldsymbol{P}, \qquad \bar{T} = \left[\Phi_R^{(1)}, \Phi_I^{(1)}, \ldots, \Phi_R^{(N)}, \Phi_I^{(N)}\right] \tag{10}$$

The result is that the differential equations are uncoupled as the $\hat{A}$ matrix for each ω_n assumes the Jordan block diagonal form:

$$\hat{A} = (\bar{T})^{-1}\bar{A}(\bar{T}) = \begin{bmatrix} \sigma_1 & \omega_1 & 0 & 0 & 0 \\ -\omega_1 & \sigma_1 & 0 & 0 & 0 \\ 0 & 0 & \sigma_2 & \omega_2 & 0 \\ 0 & 0 & -\omega_2 & \sigma_2 & 0 \\ 0 & 0 & 0 & 0 & \text{etc.} \end{bmatrix} \tag{11}$$

By iterating on ω_n and combining the eigenvectors we may assemble a global transformation matrix $\bar{T}$. Similarly, global matrices $\hat{A}$ and $\hat{B}$ are assembled from rows and columns corresponding to each eigenvalue. In a strict sense, the equality expressed by Eq. (11) is invalid in this global system because the eigenvectors that form the transformation matrix are not necessarily orthogonal. The equation is a good approximation, however, and experience has shown that if the off-diagonal terms were computed, they would be orders of magnitude smaller than the block diagonal elements.

We note that the transformed EOMs are derived from a series of approximations to the aerodynamic force. These equations have significantly higher accuracy than those based on a single linear representation over the full frequency band. The added accuracy is obtained without introducing lag terms or increasing the number of equations to be solved. We also observe that the p transform is analogous to the p-k flutter solution process described in Ref. 21 and that the eigenvalues in Eq. (11) are identical to the flutter roots computed in the MSC-NASTRAN computer program.

The elements of the input $\hat{B}$ matrix (for control surface motion as well as for atmospheric turbulence) are generated using the same first-order aerodynamic approximation that is applied for the $\hat{A}$-matrix terms. This approximation yields accurate rigid-body and flexible-mode responses (accelerations, rates, and displacements) which all depend on the aircraft states alone. The same level of accuracy, however, may not be obtainable for the external loads caused by turbulence because they are a function of the gust-induced airflow as well as the structural motion. For calculation of these loads a phase-shifted RFA[10,11] may be required to account for the effects of gust penetration. Further work is planned to evaluate the accuracy in this area of application.

Transformation to Body Axis System

For the case of longitudinal motion, the mean axis degrees of freedom ($n = 1, 2, 3$) are defined by

$$\varepsilon_1 = f, \qquad \varepsilon_2 = h, \qquad \varepsilon_3 = \theta \tag{12}$$

Here f represents fore-and-aft motion, h denotes plunge motion relative to the MFP axes, and θ symbolizes pitch about a reference axis located near the center of gravity. It should be noted that the body axis system ($\bar{X}$, $\bar{Y}$, $\bar{Z}$) used in this paper differs from the conventional one[22] in that $\bar{X}$ is positive aft and $\bar{Z}$ positive up. As a consequence, the f and θ degrees of freedom are the same whether measured in the MFP axes system or in the body axes system. The transformation between the two systems is ruled by the equation

$$\dot{h} = w + U\theta \tag{13}$$

where w is the normal velocity measured in the body axis system. In combination with the mean flow velocity U, the normal velocity induces an angle of attack measured at the pitch reference axis.

The transformation converts the vector of generalized rate coordinates $\dot{\varepsilon}$ into

$$\dot{e} = (u, w, q, \dot{\varepsilon}_4, \ldots, \dot{\varepsilon}_N) \tag{14}$$

As a result of the transformation, the aerodynamic increments

$$\Delta\mu_{m,n} = \begin{cases} \bar{q}\,\omega^{-2}\alpha_{m,n} & n = 1, 2 \\ \bar{q}\,\omega^{-2}(\alpha_{m,3} + U\beta_{m,2}) & n = 3 \end{cases} \tag{15}$$

are added to the mass matrix for all values of m. Similarly, the terms

$$\Delta\alpha_{m,n} = \alpha_{m,n} \qquad \text{for} \qquad n = 1, 2, 3 \tag{16}$$

are subtracted from the real parts of the aerodynamic matrices for all values of m ($m = 1, 2, \ldots, N$) and the terms

$$\Delta\beta_{m,3} = \begin{cases} U\omega^{-2}\alpha_{m,n} & m \neq 2 \\ U\left(\omega^{-2}\alpha_{2,2} + M/\bar{q}\right) & m = 2 \end{cases} \tag{17}$$

are subtracted from the imaginary parts. In Eq. (17) the term for $m = 2$ includes the aircraft total mass M.

As expected, all aerodynamic forces due to the coordinate displacements $\boldsymbol{e}_n$ ($n = 1, 2, 3$) are eliminated from the body axis equations. Because we assumed horizontal flight and small displacements in the original MFP formulation, the gravity component due to θ does not appear either. We observe that the aerodynamic term $\bar{q}\alpha_{2,2}/\omega^2$ is added to the aircraft mass in the vertical force equation [$m = 2$ in Eq. (15)]. This term varies slowly with frequency and at the quasi-steady limit it assumes a finite, nonzero value that is proportional to the lift derivative with respect to the $\dot{w}$ variable. In the MFP axis formulation, however, the corresponding term varies rapidly at low frequency (it is proportional to ω^2), where it causes a numerical convergence problem in the eigenvalue solution. As a consequence, we find that in practical applications the body axis formulation yields more accurate converged eigenvalues in the low-frequency range where the short-period mode is prominent.

The first-order differential equations in the body axes system may be written in the following form:

$$\dot{z} = \tilde{A}(\omega)z + \tilde{B}(\omega)\delta \tag{18}$$

where the transposed state vector is defined by

$$z^T = (u, w, q, \theta, \dot{\varepsilon}_4, \ldots, \dot{\varepsilon}_N, \varepsilon_4, \ldots, \varepsilon_N) \tag{19}$$

We note that all mean axis degrees of freedom have been placed in the first four positions and that the displacement coordinates e_1 and e_2 have been eliminated from the state vector. The θ coordinate is retained because it produces a gravity term in the nonhorizontal flight case.

With the approach described in the preceding section, the eigenvectors of the $\tilde{A}$ matrices are computed in an iterative manner to form a matrix T that is used to generate the following p-transformed matrices:

$$\hat{A} = T^{-1}\tilde{A}T, \qquad \hat{B} = T^{-1}\tilde{B} \tag{20}$$

Theoretically these system matrices ($\hat{A}$, $\hat{B}$) are identical to the ones derived from $\bar{A}$ and $\bar{B}$ in the preceding section because the eigenvalues and eigenvectors are unchanged when converting from the MFP to the body axes coordinates. However, because of a more accurate treatment of the $\dot{w}$ terms, the two sets will differ by a small amount. In the following we assume the system matrices to be derived from $\hat{A}$ and $\hat{B}$.

The antisymmetric case may be treated in an equivalent manner by performing a transformation from the MFP axes coordinates:

$$\boldsymbol{\eta} = (\dot{\varepsilon}, \varepsilon), \qquad \varepsilon = (\phi, g, \psi, \varepsilon_4, \ldots, \varepsilon_N) \tag{21}$$

to the body axis system:

$$z^T = (p, v, r, \phi, \dot{\varepsilon}_4, \ldots, \dot{\varepsilon}_N, \varepsilon_4, \ldots, \varepsilon_N) \tag{22}$$

by application of the equations

$$\dot{g} = v - U\psi, \qquad \dot{\phi} = p, \qquad \dot{\psi} = r \tag{23}$$

Derivation of Quasi-Steady Equations

Current methods for computing the aerodynamic forces generally do not permit calculation of lift forces because of changes in forward velocity or drag forces. Because of these deficiencies, the EOMs need to be modified so that the Phugoid response, for instance, can be predicted. Another reason for changing the EOMs is to account for nonlinear effects in the mean axis response. As outlined in the introduction, we propose to perform the modification by replacing our quasi-steady equations with the simulation function G_{NL}. Because these equations are supplied in physical coordinates, we need to perform a transformation back to the body axis motion variables:

$$A = T\hat{A}T^{-1}, \qquad B = T\hat{B} \tag{24}$$

Like each of the original $\tilde{A}$ matrices, the global A matrix contains coupling terms that define interactions between the dynamic modes and the rigid-body equations. The quasi-steady part of the equations may be obtained from

$$A_{\mathrm{QS}} = A_{\mathrm{RR}} + A_{\mathrm{AE}}, \qquad B_{\mathrm{QS}} = B_{\mathrm{RC}} + B_{\mathrm{AE}} \tag{25}$$

where A_{RR} and B_{RC} are submatrices of A and B corresponding to the rigid-body degrees of freedom (R) and a set of control input coordinates (C). The aeroelastic increments A_{AE} and B_{AE} are obtained by static residualization (Guyan[23] reduction):

$$A_{\mathrm{AE}} = A_{\mathrm{RD}}(A_{\mathrm{DD}})^{-1}A_{\mathrm{DR}}, \qquad B_{\mathrm{AE}} = A_{\mathrm{RD}}(A_{\mathrm{DD}})^{-1}B_{\mathrm{DC}} \tag{26}$$

The matrices A_{RD}, A_{DD}, and A_{DR} are defined as submatrices of A associated with the two coordinate sets that represent dynamic (D) and rigid (R) degrees of freedom. Similarly the B_{DC} matrix is made up of terms that couple dynamic degrees of freedom (D) to the control inputs (C).

Identification of Dynamic Increment

As stated in the preceding section, we intend to replace the quasi-steady aeroelastic portions of the A and B matrices with nonlinear equations from the nonlinear simulation. For this purpose we write the system matrices in Eq. (24) in the following form:

$$A = A_{\mathrm{RR}} + A_{\mathrm{DYN}}, \qquad B = B_{\mathrm{RC}} + B_{\mathrm{DYN}} \tag{27}$$

Here A_{DYN} contains all of the terms associated with the dynamic modes, including the coupling with rigid-body degrees of freedom. Similarly, the matrix B_{DYN} consists of terms that couple dynamic modes with the control inputs δ, as well as terms that couple dynamic control inputs ($\dot{\delta}$ and $\ddot{\delta}$) with the rigid-body modes. From Eq. (25) we obtain

$$A = A_{\mathrm{QS}} - A_{\mathrm{AE}} + A_{\mathrm{DYN}}, \qquad B = B_{\mathrm{QS}} - B_{\mathrm{AE}} + B_{\mathrm{DYN}} \quad (28)$$

The linear dynamic increments discussed in the introduction are obtained simply by identification of Eq. (2) with Eq. (28), yielding

$$\Delta G_{\mathrm{A}} = A_{\mathrm{DYN}} - A_{\mathrm{AE}}, \qquad \Delta G_{\mathrm{B}} = B_{\mathrm{DYN}} - B_{\mathrm{AE}} \quad (29)$$

Discussion of Results

The present method was validated through comparison with alternative solution techniques. A verification of the state-space EOM was obtained by generating the eigenvalue solution (prior to the integration of the dynamic equations with the nonlinear QSAE) and comparing the results with the MFP axes solution derived from the MSC-NASTRAN computer program.[21] Table 1 presents the two sets of data for an advanced transport aircraft flying at a Mach number of 0.65. We note that the low-frequency roots (for modes 2 and 3) are different but that the structural dynamic roots are practically identical. As discussed in the section following Eq. (17), the current body axes formulation is considered to yield more accurate solutions in the low frequency range than the MFP axes equations.

Another form of validation was obtained by comparing frequency response data generated by the current time-domain method with results derived from a direct solution in the frequency domain. Figures 1 and 2 show representative solutions for the magnitude and phase of two load factor responses because of horizontal tail excitations at the same flight condition that was used in the eigenvalue comparison but for a somewhat different configuration. Some minor difference in the phase is observed in parts of the spectrum where the magnitude is small, particularly for the center of gravity response (Fig. 2). As expected, no differences are discernible at the modal frequencies where the aerodynamic approximation is exact.

Time response comparisons were performed with a RFA technique developed by Tiffany and Adams.[24] Representative results are shown in Fig. 3 for the same configuration and flight condition used in the frequency response comparison. The illustrated response was computed for a horizontal tail doublet input of ±2 deg amplitude and a 5-s period starting at 2.5 s. We note that correlation between the two methods is excellent for both the mean axis data and the dynamic aeroelastic response. Another illustration of the correlation between the two methods is presented in Fig. 4 that shows the aeroelastic root locations of the system. The two sets of roots are practically identical near the imaginary axis.

Several tests were performed to verify that the present method was implemented correctly in the simulation. One such test compared the roots of the linear model with roots obtained from the simulation when it was linearized at the trim point. Various response variables were computed at the static trim condition to demonstrate that they

Table 1 Comparison of MFP and body axes solutions

	Nastran solution		Present method	
Mode	Frequency, Hz	Damping ratio	Frequency, Hz	Damping ratio
1	0.000	0.0000	0.000	0.0000
2	0.001	−0.0058	0.000	0.0000
3	0.074	0.8850	0.044	0.9498
4	1.491	0.0306	1.491	0.0306
5	1.693	0.0742	1.693	0.0741
6	2.019	0.0373	2.019	0.0374
7	2.447	0.1549	2.448	0.1552
8	2.675	0.0325	2.675	0.0325
9	2.691	0.0160	2.691	0.0160
10	3.133	0.0614	3.133	0.0612
11	3.959	0.0568	3.959	0.0568
12	4.955	0.0192	4.955	0.0191
13	5.132	0.0208	5.132	0.0209
14	5.246	0.0448	5.246	0.0448
15	6.180	0.0845	6.180	0.0843
16	6.547	0.0455	6.549	0.0455
17	7.240	0.0463	7.240	0.0462
18	7.564	0.0768	7.565	0.0767
19	8.572	0.0239	8.572	0.0239
20	9.117	0.0225	9.117	0.0226

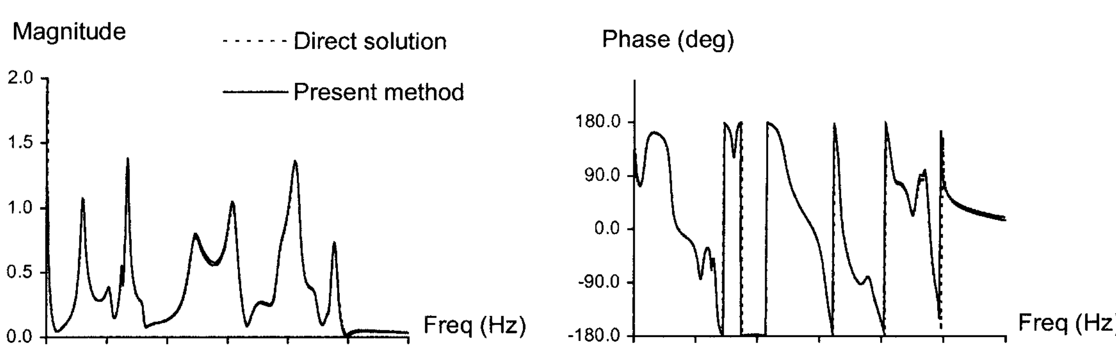

Fig. 1 Magnitude and phase comparison of pilot station load factor caused by horizontal tail excitation.

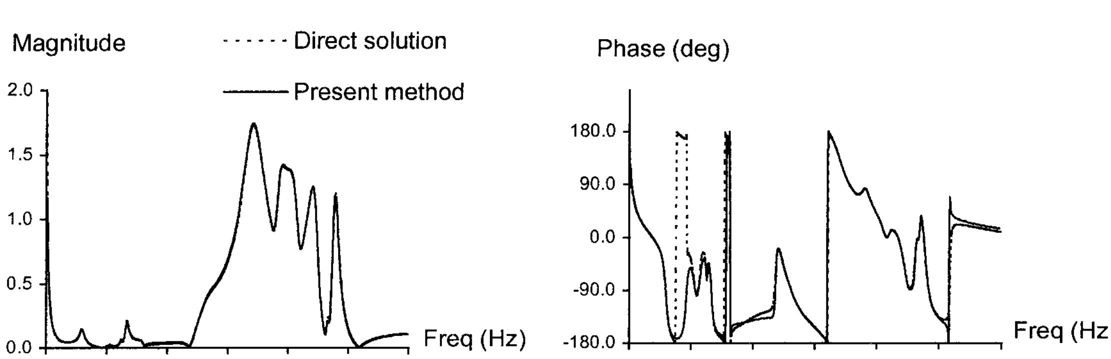

Fig. 2 Magnitude and phase comparison of center of gravity load factor caused by horizontal tail excitation.

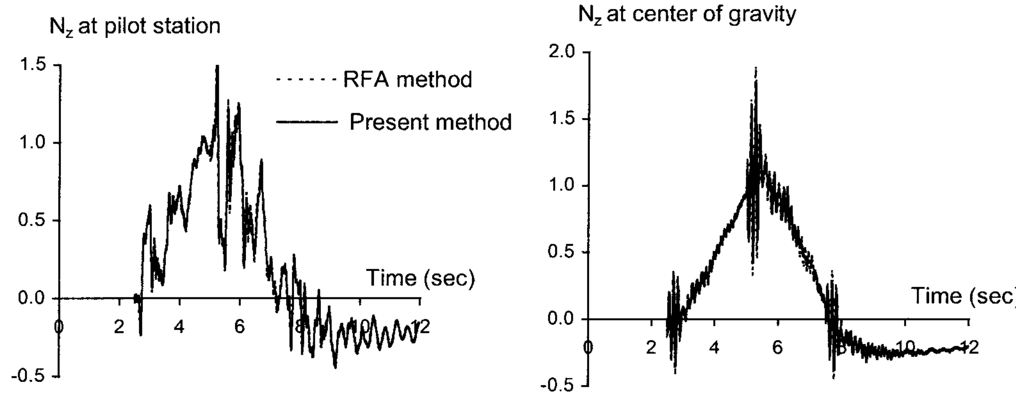

Fig. 3 Comparison of time responses caused by horizontal tail doublet input.

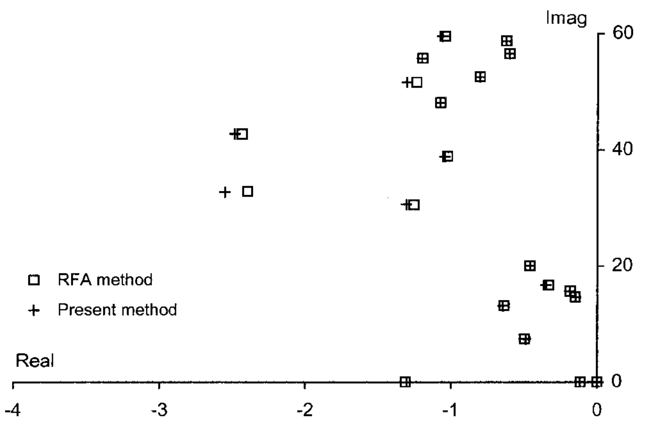

Fig. 4 Comparison of root locations for RFA method and present method.

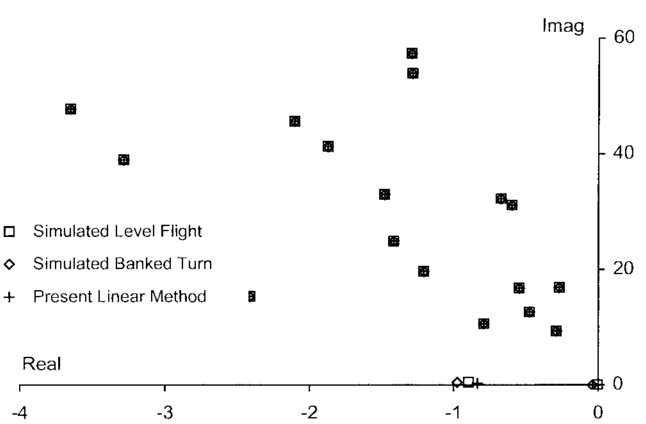

Fig. 5 Longitudinal root locations for linear analysis and two simulation analyses.

were unaffected by the dynamic increments. Figure 5, showing the roots associated with longitudinal motion, confirms that eigenvalues of the flexible modes in the linear analysis are close to the ones obtained for the simulation model at a banked turn, as well as at a level flight condition. The differences observed for the rigid-body modes are explained by differences in the trim condition for the simulation model and by the fact that the linear model uses a QSAE partition that is based on theoretical aerodynamics. A similar correlation was obtained for roots associated with lateral motion.

Conclusion

Our solution to the problem of supplying an efficient procedure for real-time simulations is based on a unique formulation that eliminates the need for auxiliary state variables to represent the unsteady aerodynamics. The solution includes transformations to a body axes coordinate system and integration of the structural dynamic equations with the quasi-steady, nonlinear equations of motion. The unified equations, which accurately preserve the roots of the dynamic aeroelastic system, have provisions for control surface inputs and atmospheric turbulence excitation. Comparisons with other solution techniques were used to validate the method. Our analytical results demonstrate excellent correlation with structural response data (accelerations, rates, and displacements) that were derived from the RFA method. Further work is required to evaluate the accuracy of external loads generated by turbulence.

Acknowledgments

The authors wish to thank W. M. Adams, NASA Langley Research Center, for helpful discussions on the theoretical development and for his assistance in the analytical validation. We also wish to express our appreciation to Dennis Henderson and Paul Kubiatko of the Boeing A&T Stability, Control and Flying Qualities Department for providing input to the validation effort and to Eugene Lavretsky of the same department for development of the simulation program.

References

[1]Rodden, W. P., and Love, J. R., "Equations of Motion of a Quasi-Steady Flight Vehicle Utilizing Restrained Static Aeroelastic Characteristics," *Journal of Aircraft*, Vol. 22, No. 9, 1985, pp. 802–809.

[2]Winther, B. A., Hagemeyer, D. A., Britt, R. T., and Rodden, W. P., "Aeroelastic Effects on the B-2 Maneuver Response," *Journal of Aircraft*, Vol. 32, No. 4, 1995, pp. 862–867.

[3]Sevart, F. D., "Development of Active Flutter Suppression Wind Tunnel Testing Technology," Air Force Flight Dynamics Lab., TR-74-126, Dayton, OH, Jan. 1975.

[4]Vepa, R., "On the Use of Pade Approximants to Represent Aerodynamic Loads for Arbitrary Small Motions of Wings," AIAA Paper 76-17, 1976.

[5]Edwards, J. W., "Unsteady Aerodynamic Modeling and Active Control," Stanford Univ., SUDAAR 504, Stanford, CA, Feb. 1977.

[6]Roger, K. L., "Airplane Math Modeling Methods for Active Control Design," CP-228, AGARD, Aug. 1977.

[7]Richardson, J. R., "A More Realistic Method for Routine Flutter Calculations," AIAA Symposium on Structural Dynamics and Aeroelasticity, Boston, MA, Aug.–Sept. 1965, pp. 10–17.

[8]Karpel, M., "Design of Active and Passive Flutter Suppression and Gust Alleviation," Ph.D. Dissertation, Stanford Univ., Stanford, CA, 1980.

[9]Pitt, D. M., and Goodman, C. E., "FAMUSS: A New Aeroservoelastic Modeling Tool," *Proceedings of the AIAA/ASME/ASCE/AHS/ASC 33rd Conference on Structures, Structural Dynamics, and Materials*, AIAA, Washington, DC, 1992, pp. 1887–1897.

[10]Dykman, J., "An Approximate Transient Gust Force Derived from Phase Shifted Rational Function Approximations to the Doublet-Lattice Harmonic Gust Coefficients," McDonnell Douglas, Rept. MDC-92-K0283, Long Beach, CA, Feb. 1992.

[11]Goggin, P. J., "A General Gust and Maneuver Load Analysis Method to Account for the Effects of Active Control Saturation and Nonlinear Aerodynamics," AIAA Paper 92-2126, April 1992.

[12]Hall, K. C., "Eigenanalysis of Unsteady Flows About Airfoils, Cascades, and Wings," *AIAA Journal*, Vol. 32, No. 12, 1994, pp. 2426–2432.

[13]Florea, R., and Hall, K. C., "Reduced Order Modeling of Unsteady Flows About Airfoils," *ASME Aeroelasticity and Fluid-Structure Interaction Problems*, Vol. AD-44, American Society of Mechanical Engineers, New York, Nov. 1994, pp. 49–68.

[14]Romanowski, M., and Dowell, E. J., "Using Eigenmodes to Form an Efficient Euler Based Unsteady Aerodynamics Analysis," *ASME Aeroelasticity and Fluid-Structure Interaction Problems*, Vol. AD-44, American Society of Mechanical Engineers, New York, Nov. 1994, pp. 147–160.

[15]Baker, M. L., Mingori, D. L., and Goggin, P. J., "Approximate Subspace Iteration for Constructing Internally Balanced Reduced Order Models of Unsteady Aerodynamic Systems," *Proceedings of the AIAA/ASME/ASCE/AHS/ASC 37th Conference on Structures, Structural Dynamics and Materials*, AIAA, Reston, VA, 1996, pp. 1070–1085.

[16]Albano, E., and Rodden, W. P., "A Doublet-Lattice Method for Calculating Lift Distributions on Oscillating Surfaces in Subsonic Flow," *AIAA Journal*, Vol. 7, No. 2, 1969, pp. 279–285.

[17]Giesing, J. P., Kalman, T. P., and Rodden, W. P., "Subsonic Unsteady Aerodynamics for General Configurations," Air Force Flight Dynamics Lab., Rept. AFFDL-TR-71-5, Dayton, OH, Nov. 1971.

[18]Heimbaugh, R. M., "Flight Controls Structural Dynamics IRAD," McDonnell Douglas, Rept. MDC-J2303, Long Beach, CA, March 1983.

[19]Duncan, W. J., "The Principles of the Galerkin Method," Aeronautical Research Council, Repts. and Memoranda, 1848, London, Sept. 1938.

[20]Lavretsky, E., "High Speed Civil Transport (HSCT) Flight Simulation and Analysis Software Development," AIAA Paper 98-0173, Jan. 1998.

[21]Rodden, W. P. (ed.), "MSC/NASTRAN Handbook for Aeroelastic Analysis," MacNeal-Schwendler Corp., MSR-57, Los Angeles, CA, Nov. 1987.

[22]Etkin, B., *Dynamics of Flight*, Wiley, New York, 1959.

[23]Guyan, R., "Reduction of Stiffness and Mass Matrices," *AIAA Journal*, Vol. 3, No. 2, 1965, pp. 380–388.

[24]Tiffany, S. H., and Adams, W. H., "Nonlinear Programming Extensions to Rational Function Approximation Methods for Unsteady Aerodynamic Forces," NASA TP 2776, July 1988.